J. Fluid Mech. (1976), *vol.* 75, *part* 3, *pp.* 593–607
Printed in Great Britain

The discrete-cilia approach to propulsion of ciliated micro-organisms

By N. LIRON AND S. MOCHON
Department of Applied Mathematics, The Weizmann Institute of Science, Rehovot, Israel

(Received 1 December 1975)

The discrete-cilia approach, or cilia sublayer model, is considered for propulsion of ciliated micro-organisms. Natural periodicity assumptions enable us to obtain a readily usable expression for the velocity where dependences on the direction of propulsion of the metachronal wave and on the time are not averaged out. Thus instantaneous interaction of the cilia with the fluid is calculable, and time-dependent velocity profiles are obtained. Calculations show that the velocity above the cilia sublayer is time independent and uniform. Closer to the bases fluid velocity fluctuations are large.

1. Introduction

The problem of the moving of fluid by cilia has been given a great deal of attention in recent years in order to try to understand how the ciliary motion performs its function, whether it be propulsion of micro-organisms to which cilia are attached, or movement of fluids and particles through pipes whose walls are covered by cilia. A description and a discussion of ciliary motion together with an extensive bibliography can be found in Blake & Sleigh (1974), who describe the two models used to portray the motion of the cilia. The first is the envelope model, on which a considerable amount of work has been done. At velocities found in nature the envelope approach is concluded by Blake & Sleigh to be a valid model only for micro-organisms which exhibit symplectic metachronism. It is not valid, for instance, for the antiplectic metachronism exhibited by many organisms. (The reader is referred to Blake & Sleigh's review and references therein for more details.)

The drawbacks of the envelope model led recently to the so-called 'cilia sublayer model', initiated by Blake (1972). In this second approach each cilium is regarded as an elongated body (slender body), and its interaction with surrounding fluid is along the lines of the now classical Gray & Hancock (1955) theory for flagella. Modifications have to be introduced to account for surfaces and for the interaction effects of all other cilia on the cilium under consideration. It is this model that we shall study in more detail. Since this model treats each cilium as a separate entity, adding up contributions to get the net effect, rather than taking the continuous envelope approach, we prefer to emphasize the contrast with the latter approach, and we call our model the discrete-cilia model.

The first to try a model of discrete cilia were Barton & Raynor (1967). They

took each cilium to be a rigid rod rotating around its base. The length of the cilium was assumed to be shorter during the recovery stroke than during the beat (in order to produce a net directional thrust). No account was taken of the metachronal wave, and each cilium was given a range of influence. This was used for a model of the movement of mucus in the trachea. Later Blake (1972) gave a much more realistic presentation, approximating each cilium by a distribution of force singularities. By considering an infinite plane sheet onto which a regular array of cilia were attached, allowing for a metachronal wave and summing over all cilia, he obtained an expression for the resultant velocity of the fluid. (Superposition is allowed since this is a linear problem, at zero Reynolds number.) The unknowns are the strengths of the force singularities on each cilium. In order to bypass the problem of finding the unknown strengths, Blake derived an approximation to the mean velocity that depends only upon the height above the infinite sheet (the x_3 co-ordinate). He then related the velocity of a cilium and the force it exerts by a modified Gray & Hancock approach. By inserting this into the expressions for the velocities of the cilium and the mean flow, and imposing the condition that on the cilium the velocity is the observed one (a kinematic description), Blake ended up with a couple of integral equations which can be solved numerically. (A much nicer description of this procedure is given by Lighthill 1975, chap. 6.)

In essence, Blake confined his attention to the interaction between a cilium and the mean flow. (The mean was taken both in a plane parallel to the sheet and in time.) This may be a good approximation near the top of the layer of cilia, where observations show only small perturbations from the mean flow, but further down deviations are large. Since the force exerted by a cilium that beats in a certain fashion depends on the relative velocity of fluid and cilium, the instantaneous velocity has to be considered rather than the mean velocity. Also the dependence on the direction of the metachronal wave (the x_1 direction) should not be averaged out.

Here we overcome the drawbacks of Blake's approach, and present a readily usable expression for the velocity. We average only in the direction perpendicular to the metachronal wave, i.e. in the direction in which all cilia are in phase (the x_2 direction). We solve directly for the strength of the force singularities, without employing the Gray & Hancock theory. A discussion of the results and a comparison with Blake's results are given in the last section.

2. The model: array of cilia

For ease of following this paper, we shall 'borrow' Blake's notation as far as possible. We consider a regular array of cilia bases on the infinite plane defined by $x_3 = 0$, (x_1, x_2, x_3) being Cartesian co-ordinates. The spacing between cilia is a in the x_1 direction and b in the x_2 direction, and we suppose that the cilia beat (essentially) in the direction of increasing x_1. We shall assume that a metachronal wave is propagating in the (positive or negative) x_1 direction such that all cilia having the same value of x_1 are in phase with each other. Thus we are modelling either symplectic or antiplectic metachronism. It is important to note that each

and every cilium goes through exactly the same cyclic motion; the only difference may be a phase difference. Define the co-ordinates of the centre-line of the cilium at the origin (which we may choose arbitrarily in the plane $x_3 = 0$) as

$$\boldsymbol{\xi}(s,t) = (\xi_1(s,t), \xi_2(s,t), \xi_3(s,t)), \quad 0 \leqslant s \leqslant L, \quad 0 \leqslant t \leqslant T, \tag{2.1}$$

where s measures the length of the cilium's centre-line from its base and t is the time. For a fixed s, the ξ_i are periodic with period T.

We now model the metachronal wave as follows: the co-ordinates of the centre-line of a cilium based at the point $(ma, nb, 0)$ at time t are given by

$$\boldsymbol{\xi}'_{m,n}(s,t) = (ma + \xi_1(s,\tau_m), nb + \xi_2(s,\tau_m), \xi_3(s,\tau_m)), \tag{2.2}$$

where

$$\tau_m = \kappa(ma) \pm \sigma t. \tag{2.3}$$

The metachronal wave is symplectic when we use the minus sign in (2.3) and antiplectic when the plus sign is used. Thus the metachronal wave has velocity $c = \sigma/\kappa$, wavelength $2\pi/\kappa$ and frequency $\sigma/2\pi$. The period $T = 2\pi/\sigma$.

If $G_j^k(\mathbf{x}, \boldsymbol{\xi})$, $j = 1, 2, 3$, is the velocity (Green's function) at $\mathbf{x}$ for a Stokeslet situated at $\boldsymbol{\xi}$ pointing in the k direction ($k = 1, 2, 3$; Cartesian co-ordinates) and such that the no-slip condition is satisfied on the plane $x_3 = 0$, then the total velocity induced by all cilia is given by

$$u_j(\mathbf{x}, t) = \sum_{n=-\infty}^{\infty} \sum_{m=-\infty}^{\infty} \int_0^L F_k(\boldsymbol{\xi}'_{m,n}(s,t))\, G_j^k(\mathbf{x}, \boldsymbol{\xi}'_{m,n}(s,t))\, ds. \tag{2.4}$$

Here, each cilium is approximated by a distribution of Stokeslets along its centre-line of variable strengths F_k, depending on direction, position on the cilium and time. The net velocity is found by summing over all cilia. The Green's function needed here is given by Blake (1971, 1972) as

$$\begin{aligned} G_j^k(\mathbf{x}, \boldsymbol{\xi}) = \frac{1}{8\pi\mu}\Bigg[&\left\{\frac{\delta_{jk}}{r} + \frac{r_j r_k}{r^3}\right\} - \left\{\frac{\delta_{jk}}{R} + \frac{R_j R_k}{R_3}\right\} \\ &+ 2\xi_3(\delta_{k\alpha}\delta_{\alpha l} - \delta_{k3}\delta_{3l}) \frac{\partial}{\partial R_l}\left\{\frac{\xi_3 R_j}{R^3} - \left(\frac{\delta_{j3}}{R} + \frac{R_j R_3}{R^3}\right)\right\}\Bigg], \end{aligned} \tag{2.5}$$

where $\alpha = 1, 2$ and $\mathbf{r}$ and $\mathbf{R}$ are defined as

$$\left.\begin{aligned} \mathbf{r} &= (x_1 - \xi_1, x_2 - \xi_2, x_3 - \xi_3), \\ \mathbf{R} &= (x_1 - \xi_1, x_2 - \xi_2, x_3 + \xi_3), \\ r &= |\mathbf{r}|, \quad R = |\mathbf{R}|. \end{aligned}\right\} \tag{2.6}$$

Blake assumes the strength of the force singularity distribution $\mathbf{F}$ to be equal along lines parallel to the x_2 axis, but variable in the x_1 direction. How the force varies in the x_1 direction is not specified.

It is reasonable to assume that $\mathbf{F}$ varies in the x_1 direction just like the metachronal wave. In other words

$$\mathbf{F}(\boldsymbol{\xi}'_{m,n}(s,t)) = \mathbf{F}(\boldsymbol{\xi}'_{m\pm1,n}(s, t - \Delta t)). \tag{2.7}$$

This condition means that whatever force acts on the cilium based at $(ma, nb, 0)$

at time t acted on the cilium based at $((m-1)a, nb, 0)$ (for symplectic metachronism) or $((m+1)a, nb, 0)$ (for antiplectic metachronism) at time $t-\Delta t$. Here Δt is the time it takes the wave to travel a distance a, so that $\Delta t = a\kappa/\sigma$. The condition that $\mathbf{F}$ be equal along lines parallel to the x_2 axis is

$$\mathbf{F}(\xi'_{m,n}(s,t)) = \mathbf{F}(\xi'_{m,n+1}(s,t)). \tag{2.8}$$

Under these conditions we get

$$\mathbf{F}(\xi'_{m,n}(s,t)) = \mathbf{F}(\xi(s,\tau_m)), \tag{2.9}$$

which can be inserted into (2.4). This follows since conditions (2.7) and (2.8) can be written explicitly as

$$\begin{aligned}&\mathbf{F}(ma+\xi_1(s,\tau_m), nb+\xi_2(s,\tau_m), \xi_3(s,\tau_m))\\ &\quad = \mathbf{F}((m\pm 1)a+\xi_1(s,\tau_m), nb+\xi_2(s,\tau_m), \xi_3(s,\tau_m))\\ &\quad = \mathbf{F}((ma+\xi_1(s,\tau_m), (n+1)b+\xi_2(s,\tau_m), \xi_3(s,\tau_m)).\end{aligned} \tag{2.10}$$

The physical interpretation of the above conditions is that we are actually demanding a one-to-one correspondence between the flow (and forces) and the configuration of the cilium (or cilia). These are conditions on the forces themselves, which are the unknowns. It is more appropriate to assume that, because all cilia beat alike, the array is regular and periodic and there is no phase difference in the x_2 direction, the velocity is periodic with period b in the x_2 direction. For the same reasons, since there is a phase difference in the x_1 direction, the velocity in the x_1 direction is periodic with period a, but with a time difference of Δt, the time it takes the wave to travel the distance a. The following periodicity is therefore assumed:

$$\left.\begin{aligned}u_j(x_1,x_2,x_3,t) &= u_j(x_1,x_2+b,x_3,t),\\ u_j(x_1,x_2,x_3,t) &= u_j(x_1\pm a,x_2,x_3,t-\Delta t),\end{aligned}\right\} \tag{2.11}$$

$$\Delta t = a\kappa/\sigma, \tag{2.12}$$

with the plus sign for antiplectic and the minus sign for symplectic metachronism.

Conditions (2.11) and (2.12) state the simple fact that, if one looks at a point $\mathbf{x}$ at time t, one cannot distinguish it from the point $\mathbf{x}+(0,b,0)$ at the time t or the point (for symplectic metachronism, say) $\mathbf{x}+(a,0,0)$ at time $t+\Delta t$, the time at which each cilium reaches the configuration (and velocity etc.) that the cilium before it (looking in the $+x_1$ direction) was in at time t. Notice that condition (2.7) or (2.11) does not imply that $\mathbf{F}$ or $\mathbf{u}$ depends on x_1 and t only through x_1-ct. The function $u=(x-ct)\cos(2\pi x/a)$ satisfies the identity

$$u(x+a,t) = u(x,t-a/c),$$

with a and c given and fixed, and is not a wave. If we also assume a one-to-one correspondence between force distributions and velocity fields then conditions (2.11) and (2.12) are equivalent to (2.7) and (2.8); see appendix. We therefore take (2.9) and insert it into (2.4), the expression for the velocity field. We now get

$$u_j(\mathbf{x},t) = \sum_{n=-\infty}^{\infty}\sum_{m=-\infty}^{\infty}\int_0^L F_k(\xi(s,\tau_m))\, G_j^k(\mathbf{x},\xi'_{m,n})\, ds. \tag{2.13}$$

In order to simplify calculations, since for some cases b is much smaller than a

and there is no phase difference in the x_2 direction, we shall average in the x_2 direction. Because of the periodicity in the x_2 direction [see (2.11)], we get for the mean velocity

$$\begin{aligned}\bar{u}_j(x_1, x_3, t) &= (1/b)\int_0^b dx_2 \sum_{m=-\infty}^{\infty}\sum_{n=-\infty}^{\infty}\int_0^L F_k(\boldsymbol{\xi}(s,\tau_m))\, G_j^k(\mathbf{x}, \boldsymbol{\xi}'_{m,n})\, ds \\ &= (1/b)\sum_{m=-\infty}^{\infty}\int_0^L F_k(\boldsymbol{\xi}_m)\left\{\int_{-\infty}^{\infty} G_j^k(\mathbf{x}, \boldsymbol{\xi}'_{m,0})\, dx_2\right\} ds. \end{aligned} \tag{2.14}$$

Here $\boldsymbol{\xi}_m = \boldsymbol{\xi}(s, \tau_m)$, and the last line follows since $G_j^k(\mathbf{x}, \mathbf{y})$ depends on x_2 and y_2 only through their difference.

Let the wavelength be

$$\lambda = m_0 a = 2\pi/\kappa, \tag{2.15}$$

i.e. we have m_0 different 'positions' of cilia in one wavelength, and then the pattern repeats itself. Let

$$m = qm_0 + r, \quad r = 0, 1, \ldots, m_0 - 1, \quad q = 0, \pm 1, \pm 2, \ldots, \tag{2.16}$$

then $\tau_m = \kappa m a \pm \sigma t = 2\pi q + \kappa r a \pm \sigma t$. Since $\boldsymbol{\xi}$ is periodic with frequency $\sigma/2\pi$, we get

$$\xi_i(s, \tau_m) = \xi_i(s, \kappa r a \pm \sigma t) \triangleq \xi_i^r(s, t), \quad r = 0, 1, \ldots, m_0 - 1. \tag{2.17}$$

Inserting (2.17) into (2.14) we get

$$\begin{aligned}\bar{u}_j(x_1, x_3, t) &= \frac{1}{b}\sum_{r=0}^{m_0-1}\int_0^L F_k(\boldsymbol{\xi}^r)\left\{\sum_{q=-\infty}^{\infty}\int_{-\infty}^{\infty} G_j^k(\mathbf{x}, \boldsymbol{\xi}'_{qm_0+r,0})\, dx_2\right\} ds \\ &= \frac{1}{b}\sum_{r=0}^{m_0-1}\int_0^L F_k(\boldsymbol{\xi}^r)\, H_j^k(x_1 - ra, x_3, \boldsymbol{\xi}^r(s,t))\, ds, \end{aligned} \tag{2.18}$$

where the kernel H_j^k is given by

$$H_j^k(x, z, \boldsymbol{\xi}) = \sum_{q=-\infty}^{\infty}\int_{-\infty}^{\infty} G_j^k(x - qm_0 a, x_2, z, \boldsymbol{\xi})\, dx_2. \tag{2.19}$$

If we wanted also to take a mean in the x_1 direction we should get

$$\bar{\bar{u}}_j(x_3, t) = \begin{cases} \dfrac{1}{m_0 ab}\displaystyle\sum_{r=0}^{m_0-1}\int_0^L F_j(\boldsymbol{\xi}^r)\, K(x_3, \xi_3^r)\, ds, & j = 1, 2, \\ 0, & j = 3, \end{cases} \tag{2.20}$$

where K is the kernel given by Blake (1972) [see (2.22)]. If in addition we wanted to take the mean over a time period, then since all $\boldsymbol{\xi}^r$ are periodic in time with the same period, all m_0 integrands would have the same time mean, and we should get

$$U_j(x_3) = \begin{cases} \dfrac{1}{ab}\displaystyle\int_0^L \overline{F_j(\boldsymbol{\xi}(s, \pm\sigma t))\, K(x_3, \xi_3(s, \pm\sigma t))}\, ds, & j = 1, 2, \\ 0, & j = 3, \end{cases} \tag{2.21}$$

the bar denoting a time mean. The kernel K is

$$K(x_3, \xi_3) = \begin{cases} x_3, & x_3 < \xi_3, \\ \xi_3, & x_3 > \xi_3. \end{cases} \tag{2.22}$$

Notice that this is identical with Blake's result only for completely synchronized motion. For symplectic or antiplectic metachronism Blake has a weight function under the integral sign which depends on the wave, but then his expression is only an approximation. We see here that (2.21) holds for any metachronism. Indeed, this is what is to be expected. The problem is linear, so all cilia go through exactly the same cycle. Since their motion differs by only a time phase, integrating over a time period annihilates the phase differences, and one should get the same result as when they are all in complete synchrony. Also, because of incompressibility we certainly have $\bar{\bar{u}}_3(x_3, t) \equiv 0$, independent of the wave. The difference in metachronism does not manifest itself explicitly, but through the force distribution, which differs for different waves in order to achieve the same movement of the cilia as is kinematically described. This is because the force depends on the difference between the velocity of the cilium and the velocity induced by all other cilia (each moment) and different waves mean that the cilium 'sees' different induced velocities.

3. The kernel H_j^k

The expression (2.18) for the velocity is practical only if one can get an expression for H_j^k, defined in (2.19), that is amenable to calculations: this will be done in this section. H_j^k is transformed into an exponentially decreasing series, easily calculated. The final result is as follows:

$$H_1^2 = H_2^1 = H_2^3 = H_3^2 = 0, \tag{3.1}$$

$$\begin{aligned} H_j^j(x_1, x_3, \boldsymbol{\xi}) = \frac{\kappa}{2\pi\mu}\Big\{&(\delta_{j1}+\delta_{j2})\,\xi_3 + (1+\delta_{j2})\sum_{q=1}^{\infty}\cos(\eta\kappa q)\exp(-x_3 q\kappa)\sinh(\xi_3\kappa q)/\kappa q \\ &+ (\delta_{j1}-\delta_{j3})\sum_{q=1}^{\infty}\cos(\eta\kappa q)\exp(-x_3 q\kappa)\,[\xi_3\cosh\xi_3\kappa q - x_3\sinh\xi_3\kappa q] \\ &- (\delta_{j1}+\delta_{j3})\,x_3\xi_3\sum_{q=1}^{\infty}\kappa q\cos(\eta\kappa q)\exp[-(x_3+\xi_3)\kappa q]\Big\}, \\ &j = 1,2,3, \quad \xi_3 < x_3, \end{aligned} \tag{3.2}$$

where $\eta = x_1 - \xi_1$. For $x_3 < \xi_3$ interchange x_3 with ξ_3:

$$\begin{aligned} H_{1,3}^{3,1} = \frac{\kappa}{2\pi\mu}\Big\{&\sum_{q=1}^{\infty}\sin(\eta\kappa q)\exp[-(x_3+\xi_3)\kappa q]\,\xi_3(1 \pm x_3\kappa q) \\ &+ \sum_{q=1}^{\infty}\sin(\eta\kappa q)\exp(-x_3\kappa q)\,[x_3\sinh\xi_3\kappa q - \xi_3\cosh\xi_3\kappa q]\Big\}, \quad \xi_3 < x_3. \end{aligned} \tag{3.3}$$

The minus sign is for the first pair of indices and the plus sign for the second pair. Again, for $\xi_3 > x_3$ interchange x_3 and ξ_3. Note that H_j^k does not depend on ξ_2, which is as should be, and depends on x_1 and ξ_1 only through their difference.

As an example we show the derivation of one part, the terms $r^{-1} - R^{-1}$ in G_j^k; see (2.5) and (2.6). By the Lipschitz integral (see Watson 1948, p. 384)

$$\begin{aligned} \frac{1}{r} - \frac{1}{R} &= \int_0^{\infty} J_0(\rho\lambda)\,[\exp(-|x_3-\xi_3|\lambda) - \exp(-|x_3+\xi_3|\lambda)]\,d\lambda \\ &= 2\int_0^{\infty} J_0(\lambda\rho)\exp(-x_3\lambda)\sinh\lambda\xi_3\,d\lambda, \quad \xi_3 < x_3, \quad \rho^2 = (x_1-\xi_1)^2 + (x_2-\xi_2)^2. \end{aligned} \tag{3.4}$$

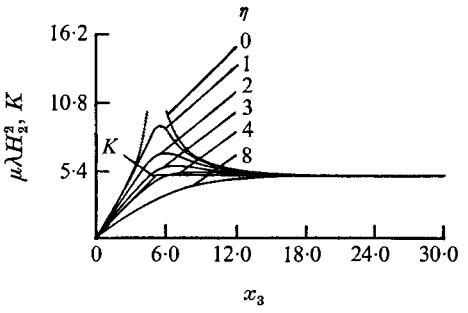

FIGURE 1. The kernel $\lambda\mu H_2^2$ *vs.* x_3 for various η, and K *vs.* x_3, for $\kappa = 0{\cdot}3$, $\xi_3 = 5{\cdot}0$. All quantities in μm. See (3.2).

For this part of $H_1^1(x_1, x_3, \boldsymbol{\xi})$ we get

$$\tilde{H}_1^1 = 2\sum_{q=-\infty}^{\infty}\int_0^{\infty}\sinh\lambda\xi_3\int_{-\infty}^{\infty}J_0\{\lambda[(x_1-qm_0a-\xi_1)^2+(x_2-\xi_2)^2]^{\frac{1}{2}}\}\,dx_2 \times\exp(-x_3\lambda)\,d\lambda. \tag{3.5}$$

Since

$$\int_{-\infty}^{\infty}J_0[\lambda(x^2+y^2)^{\frac{1}{2}}]\,dy = \frac{2}{\lambda}\cos\lambda x \tag{3.6}$$

(see Watson 1948, p. 417), we get

$$\tilde{H}_1^1 = 4\sum_{q=-\infty}^{\infty}\int_0^{\infty}\lambda^{-1}\sinh(\lambda\xi_3)\exp(-\lambda x_3)\cos[\lambda(\eta-qm_0a)]\,d\lambda, \quad \eta = x_1-\xi_1. \tag{3.7}$$

Using Poisson's summation formula in the form

$$\kappa\sum_{q=-\infty}^{\infty}f(\kappa q) = \sum_{q=-\infty}^{\infty}\int_{-\infty}^{\infty}f(\lambda)\exp\left(-2\pi i\frac{\lambda}{\kappa}q\right)d\lambda, \tag{3.8}$$

we can write

$$\begin{aligned}\tilde{H}_1^1 &= 2\sum_{q=-\infty}^{\infty}\int_{-\infty}^{\infty}\lambda^{-1}\sinh(\lambda\xi_3)\exp(-|\lambda|x_3)\cos[\lambda(\eta-m_0aq)]\,d\lambda\\ &= 2\sum_{q=-\infty}^{\infty}\int_{-\infty}^{\infty}\lambda^{-1}\sinh(\lambda\xi_3)\exp(-|\lambda|x_3)\cos(\lambda\eta)\exp\left(-2\pi i\frac{\lambda}{\kappa}q\right)d\lambda\\ &= 2\kappa\sum_{q=-\infty}^{\infty}(q\kappa)^{-1}\sinh(\xi_3\kappa q)\exp(-x_3|\kappa q|)\cos\eta\kappa q\\ &= 2\kappa\{\xi_3+2\sum_{q=1}^{\infty}(\kappa q)^{-1}\sinh(\xi_3\kappa q)\exp(-x_3\kappa q)\cos\eta\kappa q\},\end{aligned} \tag{3.9}$$

which is in the desired form.

To show the difference between the kernel H and the kernel K given by Blake (1972), we plot H_1^1, H_2^2, H_3^3 and H_1^3 compared with K in figures 1 and 2. Blake & Sleigh (1974) quote values of 1–4 Hz for the frequency and 100–400 μm/s for the velocity of the metachronal wave of *Opalina*. If we take the values 2 Hz and 100 μm/s, the wavenumber $\kappa \approx 0{\cdot}12$. For *Paramecium* Blake & Sleigh quote a value of 10 μm for the wavelength, so that $\kappa \approx 0{\cdot}63$. We shall consider a typical value of $\kappa = 0{\cdot}3$. The lengths of cilia are 10–15 μm so we shall consider values

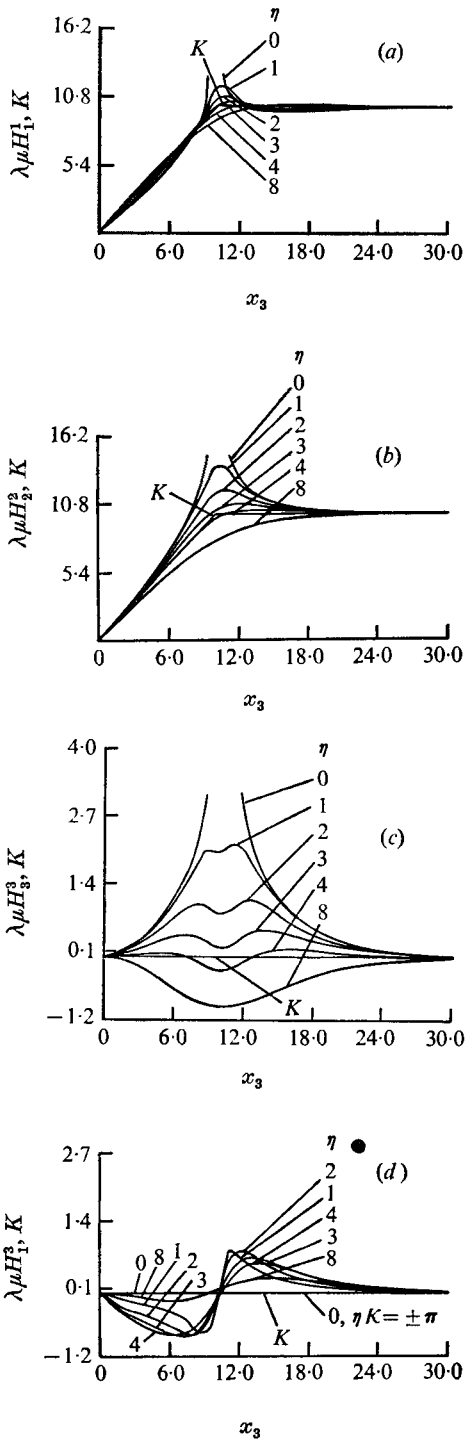

FIGURE 2. The kernels (*a*) $\lambda\mu H_1^1$, (*b*) $\lambda\mu H_2^2$, (*c*) $\lambda\mu H_3^3$ and (*d*) $\lambda\mu H_1^3$ *vs.* x_3 for various η, and K *vs.* x_3, for $\kappa = 0{\cdot}3$, $\xi_3 = 10{\cdot}0$. All quantities in μm. See (3.2).

of ξ_3 up to this range. H_3^1 lies close to H_1^3, and is closer the larger ξ_3 is. This is apparent from (3.3), so we shall not reproduce H_3^1 here. As can be seen in the plots of H_1^1 and H_2^2, K is a good approximation when x_3 is not close to ξ_3. Deviations are larger the smaller $\eta\,(=x_1-\xi_1)$. The variation with η is bounded by $\eta\kappa \leqslant \pi$ as is evident from (3.2) and (3.3). Deviations are particularly large for H_3^1 and H_3^3 compared with $K \equiv 0$ when averaged. This near-field behaviour is important in the interaction of a cilium with itself and its close neighbours. Such interaction appears in the integral equation to be solved in order to get the force distribution, equation (4.1); see the following section.

4. Integral equation for the velocity (or force)

Generally speaking, one would have to take the expression (2.13) for the velocity and demand that for every instant t and every point on every cilium the velocity matches the observed velocity. This gives an integral equation for the force densities. Blake takes the mean velocity (mean over x_1, x_2 and t) and interacts it with a cilium, using the Gray & Hancock theory to replace forces by velocities. Instead, since we are taking a mean in the x_2 direction, we shall use expression (2.18), and demand that, at time t, for every point that is on a cilium the velocity is the observed cilium velocity. Since we have taken a mean in the x_2 direction, there is no singularity. As there are m_0 different cilia in one wavelength, this should be true for all these cilia. Explicitly we therefore demand

$$\frac{\partial \xi_j^n(s,t)}{\partial t} = \bar{u}_j(\xi_1^n, \xi_3^n, t) = \frac{1}{b}\sum_{r=0}^{m_0-1}\int_0^L F_k[\boldsymbol{\xi}^r(s,t)]\,H_j^k(\xi_1^n - ra, \xi_3^n, \boldsymbol{\xi}^r(s,t))\,ds,$$
$$n = 0, 1, 2, \ldots, m_0 - 1, \qquad (4.1)$$

where ξ_i^r is defined in (2.17). This then is the integral equation for the force distribution, which can be solved. Once the forces are known they can be inserted into (2.18) for any x_1, x_3 and t. Of course we could follow Blake, replacing forces by appropriate velocities, and proceed from there. Details can be found in his paper. One should note that averaging in the x_2 direction does not mean that $\bar{u}_2$ is zero. $\bar{u}_2$ in fact does not vanish, if $F_2 \neq 0$, since $H_2^2 \neq 0$, and depends on x_1, x_3 and t.

Equations (2.18) and (4.1) are non-dimensionalized by taking L as the length scale, σL as the velocity scale, σ^{-1} as the time scale and $\mu\sigma L^2$ as the force scale. Equation (4.1) now becomes

$$\frac{\partial \xi_j^n(s,t)}{\partial t} = \frac{1}{2\pi B}\sum_{r=0}^{m_0-1}\int_0^1 F_k[\boldsymbol{\xi}^r(s,t)]\,\{2\pi\mu H_j^k(\xi_1^n - ra, \xi_3^n, \boldsymbol{\xi}^r(s,t))\}\,ds,$$
$$B = b/L, \quad n = 0, 1, 2, \ldots, m_0 - 1, \qquad (4.2)$$

where all quantities are non-dimensional. This equation was solved numerically, and the numerical details are discussed in the next section.

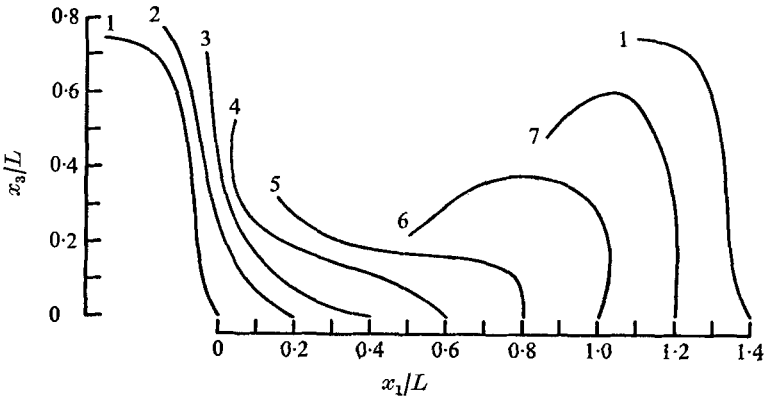

FIGURE 3. The model for the cilium beat (reproduced by the computer) for one wavelength. Increasing numbers indicate positions of the cilium in consecutive time intervals; $\lambda/L = 1{\cdot}4$.

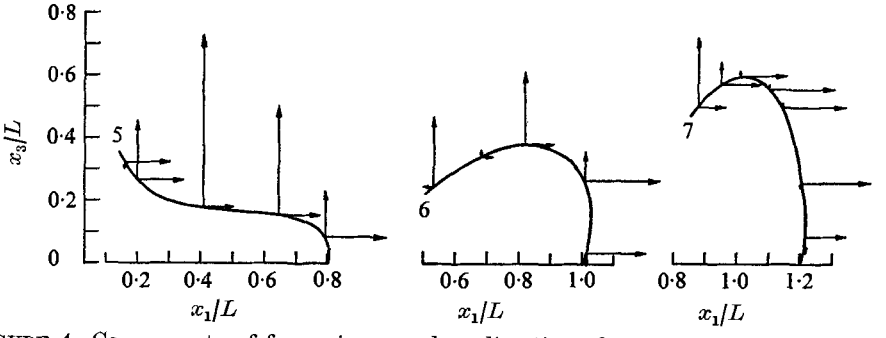

FIGURE 4. Components of forces in x_1 and x_3 directions for cilia numbers 5, 6 and 7 in figure 3. Arbitrary units.

5. Numerical results

5.1. *Description of the moving cilium*

In order to describe the moving cilium, we discretize it, taking N intervals of length $\Delta S = N^{-1}$, with the midpoint representing the interval. For a fixed point s_k, we write the periodic movement of that point as a Fourier series in time:

$$\xi_i(s_k, t) = \sum_{n=1}^{M_1} [a_{ni}(s_k)\cos nt + b_{ni}(s_k)\sin nt], \quad i = 1, 2, 3,$$
$$s_k = (k - \tfrac{1}{2})/N, \quad k = 1, 2, \ldots, N, \tag{5.1}$$

where $a_{ni}(s_k)$ and $b_{ni}(s_k)$ are found by fitting to the path of the cilium. One then extends this to

$$\xi_i(s, t) = \sum_{n=1}^{M_2} [a_{ni}(s)\cos nt + b_{ni}(s)\sin nt], \quad i = 1, 2, 3, \tag{5.2}$$

by fitting each $a_{ni}(s_k)$ and $b_{ni}(s_k)$ to a polynomial in s of order M_2;

$$a_{ni} = \sum_{m=1}^{M_2} A_{nim} s^m, \quad b_{ni} = \sum_{m=1}^{M_2} B_{nim} s^m. \tag{5.3}$$

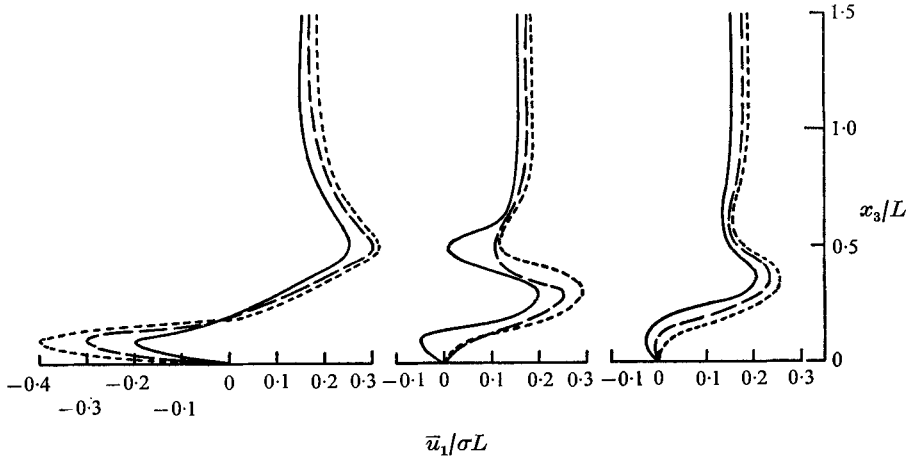

FIGURE 5. Computer calculations of velocity profiles, depending on the number of points taken along each cilium to represent it: ———, 6 points; — — —, 9 points; - - - - - -, 12 points ≃ 16 points.

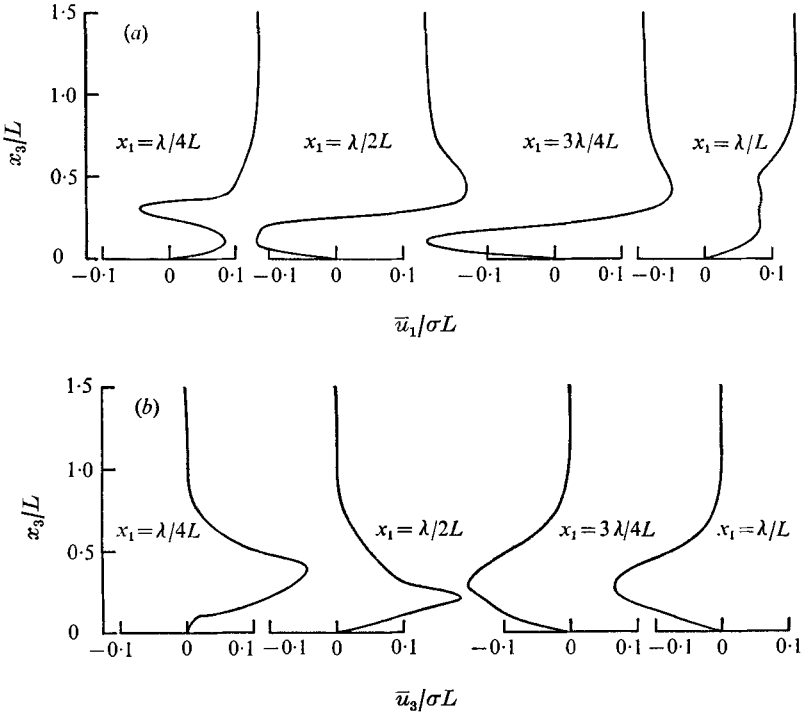

FIGURE 6. (*a*) The velocity component $\bar{u}_1(x_1, x_3)$ and (*b*) the velocity component $\bar{u}_3(x_1, x_3)$ for various values of x_1. The beat is given in figure 3.

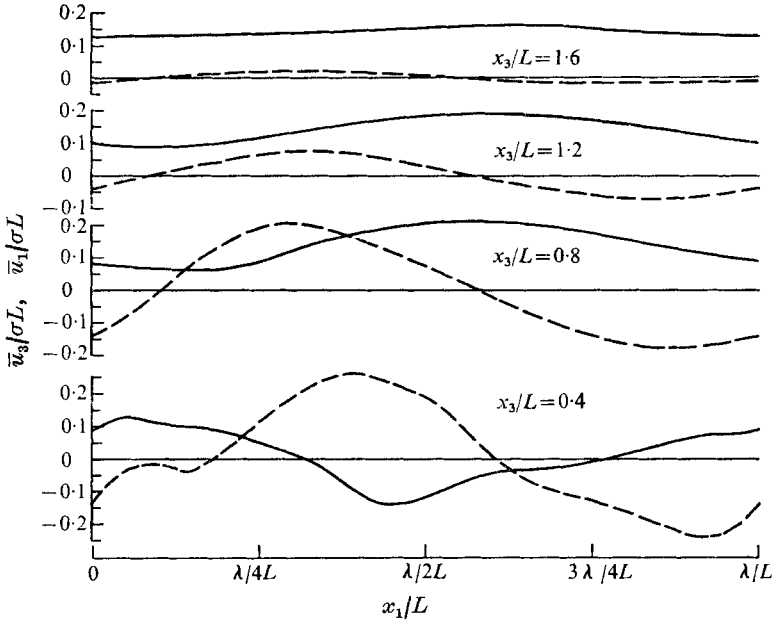

FIGURE 7. The velocities $\bar{u}_1$ (solid curves) and $\bar{u}_3$ (broken curves) *vs.* x_1 for various heights x_3 above the sheet. The beat is given in figure 3.

This is done by a least-squares procedure. In our numerical calculations we took $M_2 = 3$. Notice that this procedure is identical to that of Blake (1972). It is important in our opinion not to introduce unnecessary complications and diversity, unless absolutely necessary. In this case Blake's procedure is reasonable and there is no need for a different one.

In order to demonstrate the technique, we chose a cilium beat from Machemer (1972), which shows apparent two-dimensional antiplectic metachronism for *Paramecium*, as given in figure 3. Figure 3 shows the different cilia in one wavelength, which of course corresponds also to different positions of one cilium at fixed time intervals during one time period. Increasing numbers represent increasing time.

5.2. *Solution of integral equation*

In order to solve for the forces in (4.1), we replace the integral by a quadrature formula (we used the midpoint rule using the points s_k). We thus get a set of $3m_0N$ linear inhomogeneous equations in $3m_0N$ unknowns: the forces. The solution for the forces is exhibited in figure 4, for time steps 5, 6 and 7 of the cilium. The forces are shown in component form, the force being the vectorial sum at each point. Forces are seen to be larger during the early stages of the beat than towards the end of the beat.

5.3. *Velocity profiles*

The dependence of results on the number of points taken along the cilia is exhibited in figure 5. (This is a different beat from the one in figure 3.)

Velocity profiles $\bar{u}_1$ and $\bar{u}_3$ are given in figures 6(*a*) and (*b*). These show the

great variability in space (or time) of the velocity. Notice however that $\bar{u}_3 \to 0$ and $\bar{u}_1 \to U$, the propulsion velocity, towards the top part of the ciliary sublayer, practically independently of time and position along the wave (independently of x_1). This beat thus indeed induces uniform motion of the fluid above the cilia sublayer. The fluctuations can be seen in figure 7. These are especially large near the bottom third, being of the same order as the velocity of propulsion itself.

6. Discussion

We have presented here a model for the cilia layer which depends both on time and on distance in the direction of the metachronal wave. This was achieved by appropriate periodicity assumptions about the velocity: conditions (2.11) and (2.12). By averaging only in the x_2 direction we obtained for the velocity the expression (2.18),

$$\bar{u}_j(x_1, x_3, t) = \frac{1}{b} \sum_{r=0}^{m_0-1} \int_0^L F^k(\boldsymbol{\xi}^r)\, H_j^k(x_1 - ra, x_3, \boldsymbol{\xi}^r(s,t))\, ds, \tag{6.1}$$

compared with the expression obtained by Blake (1972),

$$\left.\begin{aligned} U_\alpha(x_3) &= \frac{1}{\mu ab}\int_0^L w(s,t)\, K(x_3, \xi_3(s,t))\, F_\alpha(\boldsymbol{\xi}(s,t))\, ds + O(ab/L^2)\,\sigma L, \quad \alpha = 1,2, \\ U_3(x_3) &= O(ab/L^2)\,\sigma L. \end{aligned}\right\} \tag{6.2}$$

Here

$$w(s,t) = \begin{cases} 1, & \text{synchronized}, \\ [1 - c^{-1}\partial\xi_1/\partial t]^{-1}, & \text{symplectic}, \\ [1 + c^{-1}\partial\xi_1/\partial t]^{-1}, & \text{antiplectic}. \end{cases} \tag{6.3}$$

K is given in (2.22) and H in §3.

There are two major differences between the above two expressions. The first concerns the kernel H as compared with K. Comparisons of H and K can be seen in figures 1 and 2. For H_3^1, H_1^3 and H_3^3, Blake's kernel is zero but ours is not; see figures 2(*c*) and (*d*). K is seen to approximate H_1^1 and H_2^2 nicely, except when $|x_1 - \xi_1|$ is of the order of ξ_3, and near $x_3 = \xi_3$. Deviation in that region may be large since $H_j^j(x_1, x_3, \xi_1, \xi_3) = \infty$. These deviations are important since the interaction of a cilium with itself and its closest neighbours falls within this region.

The second major difference is that the velocity in (6.1) consists of a sum over the different positions of the cilia in one wavelength rather than the wave-modified kernel given by Blake. It is interesting to note that, if we average our velocity expression (6.1) over x_1 and t, we obtain Blake's expression (6.2) with $O(ab/L^2) \equiv 0$ and $w(s,t) \equiv 1$ for all waves; see (2.21). Disregarding the error terms we see that our averaged velocity coincides with Blake's when $c^{-1}\partial\xi_1/\partial t$ is small. Under this condition, our velocity field is a direct extension of Blake's velocity field.

The importance of obtaining a time-dependent velocity stems from the fact that the force a cilium has to develop is directly proportional to the difference between the velocity the cilium 'sees' and the velocity it actually has (Gray &

Hancock theory), and therefore one has to look at the instantaneous velocity rather than at the mean velocity. The time-dependent velocity profiles in figures 6 and 7 confirm this, as deviations are seen to be very large, and both positive and negative. Also, the velocity in the x_3 direction in the bottom part of the cilia layer is of the same order of magnitude as the propulsion speed, whereas in Blake's approach this velocity is zero.

The calculations show that the velocity immediately above the cilia layer is uniform and almost time independent (see figure 7), as observed experimentally.

Appendix

We first show that the periodicity assumptions (2.11) and (2.12) imply conditions (2.8) and (2.7) respectively. To show (2.8) write down condition (2.11) using (2.4):

$$\begin{aligned}\mathscr{F} &\equiv \sum_{m=-\infty}^{\infty}\sum_{n=-\infty}^{\infty}\int_0^L F_k(\boldsymbol{\xi}'_{m,n}(s,t))\,G_j^k(\mathbf{x},\boldsymbol{\xi}'_{m,n}(s,t))\,ds\\ &= \sum_{m=-\infty}^{\infty}\sum_{n=-\infty}^{\infty}\int_0^L F_k(\boldsymbol{\xi}'_{m,n}(s,t))\,G_j^k(\mathbf{x}+\mathbf{b},\boldsymbol{\xi}'_{m,n}(s,t))\,ds,\end{aligned}$$

where $\mathbf{b} = (0, b, 0)$. Shifting the dummy index n by one gives

$$\mathscr{F} = \sum_{m=-\infty}^{\infty}\sum_{n=-\infty}^{\infty}\int_0^L F_k(\boldsymbol{\xi}'_{m,n+1}(s,t))\,G_j^k(\mathbf{x}+\mathbf{b},\boldsymbol{\xi}'_{m,n+1}(s,t))\,ds.$$

$G_j^k(\mathbf{x},\mathbf{y})$ depends on x_2 and y_2 is only through x_2-y_2 [see (2.5)], so that

$$\begin{aligned}\mathscr{F} &= \sum_{m=-\infty}^{\infty}\sum_{n=-\infty}^{\infty}\int_0^L F_k(\boldsymbol{\xi}'_{m,n+1}(s,t))\,G_j^k(\mathbf{x},\boldsymbol{\xi}'_{m,n+1}(s,t)-\mathbf{b})\,ds\\ &= \sum_{m=-\infty}^{\infty}\sum_{n=-\infty}^{\infty}\int_0^L F_k(\boldsymbol{\xi}'_{m,n+1}(s,t))\,G_j^k(\mathbf{x},\boldsymbol{\xi}'_{m,n}(s,t))\,ds.\end{aligned}$$

Subtracting the last line from the first, we get

$$0 \equiv \sum_{m=-\infty}^{\infty}\sum_{n=-\infty}^{\infty}\int_0^L [F_k(\boldsymbol{\xi}'_{m,n}(s,t)) - F_k(\boldsymbol{\xi}'_{m,n+1}(s,t))]\,G_j^k(\mathbf{x},\boldsymbol{\xi}'_{m,n}(s,t))\,ds.$$

By the assumption of a unique force distribution for a given velocity field, it follows that the expression in the square brackets must vanish for all m and n. This is condition (2.8).

To get (2.7) one follows similar lines, again noting that $G_j^k(\mathbf{x},\mathbf{y})$ depends on x_1 and y_1 only through their difference. Since the dependence on time is through $\boldsymbol{\xi}(s,\tau_m)$, for every m (and n) the shift of the dummy index m is cancelled by appropriately adding or subtracting $\Delta t\,(=\kappa a/\sigma)$. Thus, again assuming uniqueness, one arrives at the first part of (2.10), which is equivalent to (2.7).

To show that (2.7) and (2.8) imply (2.11) and (2.12) take the expression for the velocity (2.4) written as in (2.13), and again use the condition that $G_j^k(\mathbf{x},\mathbf{y})$ depends on x_1, y_1, x_2 and y_2 only through x_1-y_1 amd x_2-y_2 and shift the appro-

priate dummy variable summed over. For example, for symplectic metachronism

$$u_j(x_1-a, x_2, x_3, t-\Delta t) = \sum_{m=-\infty}^{\infty} \sum_{n=-\infty}^{\infty} \int_0^L F_k(\boldsymbol{\xi}(s, \kappa m a - (t-\Delta t))) \times G_j^k(x_1-a, x_2, x_3, \boldsymbol{\xi}'_{m,n}(s, t-\Delta t))\, ds.$$

Use of $\sigma \Delta t = \kappa a$, (2.2) and (2.3) and shifting m by one shows that the right-hand side equals

$$\sum_{m=-\infty}^{\infty} \sum_{n=-\infty}^{\infty} \int_0^L F_k(\boldsymbol{\xi}(s, \tau_m))\, G_j^k(\mathbf{x}-\mathbf{a}, \boldsymbol{\xi}'_{m,n}(s,t)-\mathbf{a})\, ds,$$

where $\mathbf{a} = (a, 0, 0)$, and by the invariance of G_j^k, this in turn equals

$$\sum_{m=-\infty}^{\infty} \sum_{n=-\infty}^{\infty} \int_0^L F_k(\boldsymbol{\xi}(s, \tau_m))\, G_j^k(\mathbf{x}, \boldsymbol{\xi}'_{m,n}(s,t))\, ds = u_j(\mathbf{x}, t).$$

REFERENCES

Barton, C. & Raynor, S. 1967 Analytic investigations of cilia induced mucous flow. *Bull. Math. Biophys.* **29**, 419–428.

Blake, J. R. 1971 A note on the image system for a Stokeslet in a no-slip boundary. *Proc. Camb. Phil. Soc.* **70**, 303–310.

Blake, J. R. 1972 A model for the micro-structure in ciliated organisms. *J. Fluid Mech.* **55**, 1–23.

Blake, J. R. & Sleigh, M. A. 1974 Mechanics of ciliary locomotion. *Biol. Rev.* **49**, 85–125.

Gray, J. & Hancock, G. J. 1955 The propulsion of sea-urchin spermatozoa. *J. Exp. Biol.* **32**, 802–814.

Lighthill, M. J. 1975 *Mathematical Biofluiddynamics.* Philadelphia: SIAM.

Machemer, H. 1972 Ciliary activity and origin of metachrony in *Paramecium*: effects of increased viscosity. *J. Exp. Biol.* **57**, 239–259.

Watson, G. N. 1948 *A Treatise on the Theory of Bessel Functions*, 2nd edn. Cambridge University Press.